Gap nodes induced by coexistence with antiferromagnetism in iron-based superconductors

S. Maiti,[1] R. M. Fernandes,[2,3] and A.V. Chubukov[1]

[1] *Department of Physics, University of Wisconsin, Madison, Wisconsin 53706, USA*
[2] *Department of Physics, Columbia University, New York, New York 10027, USA*
[3] *Theoretical Division, Los Alamos National Laboratory, Los Alamos, NM, 87545, USA*

(Dated: February 25, 2013)

We investigate the pairing in iron pnictides in the coexistence phase, which displays both superconducting and antiferromagnetic orders. By solving the pairing problem on the Fermi surface reconstructed by long-range magnetic order, we find that the pairing interaction necessarily becomes angle-dependent, even if it was isotropic in the paramagnetic phase, which results in an angular variation of the superconducting gap along the Fermi surfaces. We find that the gap has no nodes for a small antiferromagnetic order parameter M, but may develop accidental nodes for intermediate values of M, when one pair of the reconstructed Fermi surface pockets disappear. For even larger M, when the other pair of reconstructed Fermi pockets is gapped by long-range magnetic order, superconductivity still exists, but the quasiparticle spectrum becomes nodeless again. We also show that the application of an external magnetic field facilitates the formation of nodes. We argue that this mechanism for a nodeless-nodal-nodeless transition explains recent thermal conductivity measurements of hole-doped $(Ba_{1-x}K_x)Fe_2As_2$ [J-Ph. Read *et al* arXiv:1105.2232].

PACS numbers:

I. INTRODUCTION

Exploring the different regions in the phase diagram of iron based superconductors (FeSCs) is an important step towards developing a unified understanding of the physics of superconductivity in these systems. A typical phase diagram of a FeSC in the (T, x) plane, where x is doping, shows a metallic antiferromagnetic order, also called spin density wave (SDW), below T_N at $x = 0$. Upon doping, the SDW order parameter is suppressed and superconductivity (SC) emerges with maximum $T_c(x)$ near the point where $T_c(x)$ exceeds $T_N(x)$ (an "optimal doping"). The gap symmetry at optimal doping is most likely s^{+-}, but the structure of the s-wave gap varies from one material to another: the gap is nodeless in $Ba(Fe_{1-x}Co_x)_2As_2$ [1–3] and $(Ba_{1-x}K_x)Fe_2As_2$ [4–6], but has nodes in $BaFe_2(As_{1-x}P_x)_2$ [7,8].

In this article we investigate the behavior of the s^{+-} SC gap in the underdoped regime of the $Ba(Fe_{1-x}Co_x)_2As_2$ and $(Ba_{1-x}K_x)Fe_2As_2$ systems, where $T_c(x) < T_N(x)$, and superconductivity emerges in a continuous fashion from a pre-existing SDW order. The microscopic coexistence of SC and SDW below $T_c(x)$ has been reported by magnetization and NMR experiments[9–12].

The electronic structure of FeSCs in the paramagnetic phase consists of near-circular hole pockets and elliptical electron pockets. We assume, following earlier works[13–19], that the interaction leading to SDW order is independent on the angle along the FS[20]. In this situation, the Brillouin Zone (BZ) is reduced once the SDW order sets in, and the Fermi surface (FS) is reconstructed into four banana-like pockets (right panel in Fig. 1). As the SDW order parameter M increases, the reconstructed pockets shrink and eventually disappear. This happens

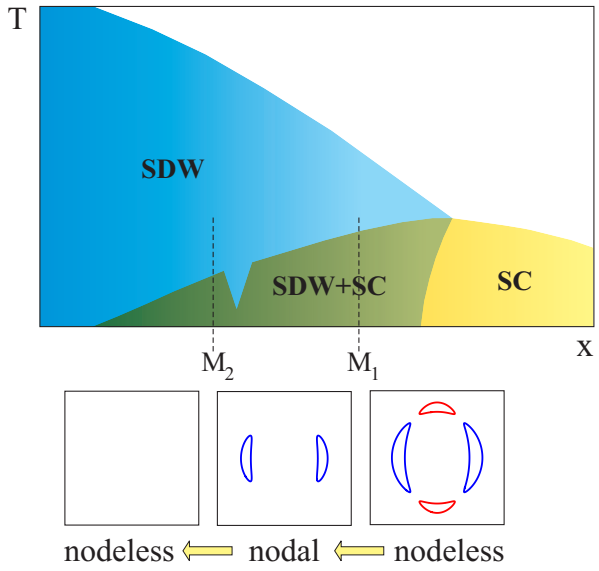

Figure 1: Schematic phase diagram showing the nodeless-nodal-nodeless transitions inside the region where superconductivity (SC) and spin density wave (SDW) coexist. Each transition is roughly associated with the disappearance of one pair of magnetically reconstructed Fermi surface pockets. M_1 and M_2 refer to the values of the SDW order parameter M at which the two pairs of pockets disappear respectively. A dip in T_c is observed near M_2, when both pockets disappear.

in two stages: first, at $M = M_1$, the number of pockets shrinks from four to two, (middle panel in Fig. 1), and then the remaining two pockets vanish at a larger value $M = M_2$ (left panel in Fig. 1). Because these reconstructed FSs are formed by mixing electron and hole bands, on which the s^{+-} SC order parameter has different signs in the absence of SDW order, one could

naively expect that the SC gap on the reconstructed FSs alternates between plus and minus signs, implying that it must have nodes. However, calculations show[13] that this is not the case because SDW order, with e.g. $\langle S_x \rangle \neq 0$, mixes hole and electron FSs with opposite σ_z components of electron spins. Because a spin-singlet s-wave gap changes sign under $\sigma_z \to -\sigma_z$, the sign change imposed by the s^{+-} gap structure is compensated by the sign change due to the flip of σ_z, and, as a result, the gaps on the reconstructed FSs retain the same nodeless structure as in the absence of magnetic order.

Experiments near the onset of the co-existence phase, where M is small, are in agreement with this reasoning. For instance, the ratio κ/T, where κ is the in-plane thermal conductivity, tends to zero in the $T \to 0$ limit, as it is expected for a superconductor with a nodeless gap. However, recent thermal conductivity measurements on $(Ba_{1-x}K_x)Fe_2As_2$ deep in the coexistence phase[22] found that there is a range of dopings where κ/T remains finite at $T = 0$, as it happens in a superconductor with line nodes. At even smaller dopings, κ/T again vanishes at $T = 0$. Application of a magnetic field makes the doping dependence more smooth and extends the range of nodal behavior.

In this article we explain the sequence of nodeless-nodal-nodeless behavior as a transition from a nodeless s^{+-} gap in the region where all four reconstructed FS pockets are present, to an s^{+-} gap with accidental nodes in the region where two FS pockets are present, to the fully gapped quasiparticle spectrum in the region where the remaining two reconstructed FS pockets are also gapped (see Fig. 1). We show that the pairing interaction in the coexistence phase acquires an additional angular dependence as it gets dressed by angle-dependent coherence factors associated with the SDW order. The angular dependence of the interactions in turn gives rise to an angular dependence of the superconducting gap. This effect is weak in the limit of small M, considered in Ref. 13, when all four reconstructed Fermi pockets are present, but is strong and gives rise to gap nodes when M becomes large enough to gap out one pair of Fermi pockets. At even larger M, deeper in the coexistence region, the remaining pair of Fermi pockets is gapped out. In this situation, superconductivity still develops over some range of dopings[14], but the quasiparticle excitation spectrum remains gapped irrespective of the structure of the SC gap, and κ/T again vanishes at $T = 0$. Concurrently, the superconducting transition temperature T_c shows a minimum when the remaining pockets vanish. The theoretical behavior across the SDW-SC coexistence region is shown schematically in Fig. 1. It agrees well with the experimental results of Refs. 22**?**

The paper is organized as follows. In Sec. II we describe the formalism listing out the details of the FS geometries, the nature of the reconstructed FSs, and the generic form of the SC gap in the coexistence region. In Sec. III we discuss the solutions for the gap obtained within this formalism, show when and how nodes arise in the coexistence region, and provide analytical explanation of the results. We also briefly discuss the role played by bands that do not participate in the formation of SDW. In Sec.IV we show that the doping range where the SC gap has nodes is enhanced by applying a magnetic field. We state our final conclusions in Sec. V.

II. THE PAIRING PROBLEM ON THE RECONSTRUCTED FERMI SURFACE

Our point of departure is a microscopic band model of interacting fermions located near hole or electron pockets. The electronic structure of FeSCs consists of two or three hole pockets, centered at $(0, 0)$ in the folded zone (two Fe atoms per unit cell), and two hybridized electron pockets centered at (π, π). The interactions between low-energy fermions are generally angle-dependent already in the normal state, before either SDW or SC order sets in, which gives rise to angle-dependent SDW and SC gaps even outside the coexistence region.

As we said, we follow earlier works and consider a simplified model in which we neglect the angular dependencies of the interactions in the normal state, and approximate the normal-state interactions as constants[13–19]. We further neglect the hybridization and perform calculations in the unfolded zone (one Fe atom per unit cell), in which electron pockets are ellipses centered at $(0, \pi)$ and $(\pi, 0)$ and hole pockets are at $(0, 0)$ and (π, π). Finally, we neglect the third hole pocket and only consider two circular hole pockets centered at $(0, 0)$ in the unfolded zone (in orbital notations these are d_{xz}/d_{yz} pockets). Earlier works have found[17] that SDW magnetic order emerges in this model with ordering vector $\mathbf{Q} = (0, \pi)$ or $\mathbf{Q} = (\pi, 0)$, mixing one hole and one electron pocket. For definiteness we set $\mathbf{Q} = (0, \pi)$ in which case one hole pocket at $(0, 0)$ and one electron pocket at $(0, \pi)$ are mixed up. The other two pockets are not participating in SDW and remain intact once the SDW order sets in. In line with our goal, we first consider only the 2-pocket model with one circular hole and one elliptical electron pocket, which get reconstructed in the SDW phase. We discuss the role of the other pockets later in the next section.

To quadratic order in the fermions, the Hamiltonian of the 2-pocket model in the SDW phase is $H_0 + H_{SDW}$, where

$$\begin{aligned} H_0 &= \sum_{\mathbf{k},\sigma} \left(\varepsilon^c_{\mathbf{k}} c^\dagger_{\mathbf{k}\sigma} c_{\mathbf{k}\sigma} + \varepsilon^f_{\mathbf{k}+\mathbf{Q}} f^\dagger_{\mathbf{k}+\mathbf{Q}\sigma} f_{\mathbf{k}+\mathbf{Q}\sigma} \right) \\ H_{SDW} &= \sum_{\mathbf{k}\sigma} M \left(\sigma c^\dagger_{\mathbf{k}\sigma} f_{\mathbf{k}+\mathbf{Q}\sigma} + \text{h.c.} \right) \end{aligned} \quad (1)$$

Here c and f are fermionic operators for hole and electron states, respectively, σ is ± 1, and M is the SDW order parameter, which we treat below as a variable. In practice, larger M correspond to smaller dopings, whereas smaller M correspond to doping close to the optimal one. The fermionic dispersions are

$$\begin{aligned} \varepsilon^c_{\mathbf{k}} &= \mu_c - \frac{k_x^2+k_y^2}{2m} \\ \varepsilon^f_{\mathbf{k}+\mathbf{Q}} &= -\mu_f + \frac{k_x^2}{2m_x} + \frac{k_y^2}{2m_y} \end{aligned} \quad (2)$$

where m, m_x, m_y are the effective band masses of the fermions. For definiteness, we set the interatomic spacing to one and use $\mu_c = \mu_f = \mu$, $m = 1/(2\mu)$, $m_x = 0.5/(2\mu)$, and $m_y = 1.5/(2\mu)$. These parameters are chosen to give the FS geometry as in Fig. 2. We will also measure M in units of 2μ.

The M term in (1) couples c and f operators such that the eigenstates of (1) are coherent superpositions of electrons and holes. These are described by new fermionic operators a and b, with dispersion $E^{a,b}_{\mathbf{k}}$ that vanishes at the reconstructed FSs. The transformation to the new operators is

$$\begin{pmatrix} \sigma a_{\mathbf{k}\sigma} \\ b_{\mathbf{k}\sigma} \end{pmatrix} = \begin{pmatrix} -\sigma\cos\theta_{\mathbf{k}} & \sin\theta_{\mathbf{k}} \\ -\sin\theta_{\mathbf{k}} & -\sigma\cos\theta_{\mathbf{k}} \end{pmatrix} \begin{pmatrix} c_{\mathbf{k}\sigma} \\ f_{\mathbf{k}+\mathbf{Q}\sigma} \end{pmatrix} \quad (3)$$

where

$$\begin{aligned} \cos\theta_{\mathbf{k}} &= \frac{M}{\sqrt{M^2+(E^-)^2}} \\ \sin\theta_{\mathbf{k}} &= \frac{E^-}{\sqrt{M^2+(E^-)^2}} \end{aligned} \quad (4)$$

and

$$E^- = \frac{\varepsilon^c - \varepsilon^f}{2} - \sqrt{\left(\frac{\varepsilon^c-\varepsilon^f}{2}\right)^2 + M^2} \quad (5)$$

such that

$$\begin{aligned} \cos 2\theta_{\mathbf{k}} &= \frac{\frac{\varepsilon^c-\varepsilon^f}{2}}{\sqrt{M^2+\left(\frac{\varepsilon^c-\varepsilon^f}{2}\right)^2}} \\ \sin 2\theta_{\mathbf{k}} &= -\frac{M}{\sqrt{M^2+\left(\frac{\varepsilon^c-\varepsilon^f}{2}\right)^2}} \end{aligned} \quad (6)$$

In terms of the new operators,

$$H_0 + H_{SDW} = \sum_{\mathbf{k},\sigma} \left(E^a_{\mathbf{k}} a^\dagger_{\mathbf{k}\sigma} a_{\mathbf{k}\sigma} + E^b_{\mathbf{k}} b^\dagger_{\mathbf{k}\sigma} b_{\mathbf{k}\sigma} \right) \quad (7)$$

where

$$E^{a,b}_{\mathbf{k}} = \frac{\varepsilon^c+\varepsilon^f}{2} \pm \sqrt{\left(\frac{\varepsilon^c-\varepsilon^f}{2}\right)^2 + M^2} \quad (8)$$

are the quasi-particle excitation energies of the SDW state (the plus sign corresponds to a fermions, the minus sign corresponds to b fermions).

The condition $E^{a,b}_{\mathbf{k}} = 0$ defines the new reconstructed FSs. For small enough M, there are two pairs of banana-shaped reconstructed pockets, the a-pockets and the b-pockets (see Fig. 2), with the latter larger than the former. At the critical $M = M_1$ given by

$$M_1 = \frac{1}{4}\frac{|m-m_y|}{\sqrt{mm_y}} \quad (9)$$

the a-pockets disappear while the b-pockets remain (Fig. 2-right). At even larger $M = M_2$ given by

$$M_2 = \frac{1}{4}\frac{|m-m_x|}{\sqrt{mm_x}} \quad (10)$$

the b-pockets also disappear, i.e. all electronic states become gapped by SDW[20]. For our set of parameters $M_1 \approx 0.102$ and $M_2 \approx 0.177$.

We now turn to the issue of the pairing on the reconstructed FS. There are four residual interactions between the original fermions located near the hole and electron FSs [19]: the interaction between fermionic densities near hole and electron pockets $\left[U_1 c^\dagger_\sigma c_\sigma f^\dagger_{\sigma'} f_{\sigma'}\right]$, the exchange interaction between hole and electron pockets $\left[U_2 c^\dagger_\sigma f_\sigma f^\dagger_{\sigma'} c_{\sigma'}\right]$, the umklapp pair-hopping interaction in which two fermions near a hole pocket are converted into two fermions near an electron pocket and vice-versa $\left[U_3/2(c^\dagger_\sigma f_\sigma c^\dagger_{\sigma'} f_{\sigma'} + f^\dagger_\sigma c_\sigma f^\dagger_{\sigma'} c_{\sigma'})\right]$, and the density-density interaction within each pocket $\left[U_4/2(c^\dagger_\sigma c_\sigma c^\dagger_{\sigma'} c_{\sigma'} + f^\dagger_\sigma f_\sigma f^\dagger_{\sigma'} f_{\sigma'})\right]$. In the absence of SDW order, only U_3 and U_4 contribute to the pairing channel (U_3 must be larger than U_4 for s^{+-} pairing). In the SDW phase, c and f operators are mixed up, and all four interactions contribute to pairing vertices for a and b fermions. The interactions U_2 and U_4 do not give rise to new physics and only renormalize the values of the pairing vertices obtained from the U_1 and U_3 terms. To shorten the formulas, we neglect the U_2 and U_4 terms and approximate H_{int} by

$$\begin{aligned} H_{int} &= \sum_{[1234]} U_1\, c^\dagger_{1\sigma} f^\dagger_{2\sigma'} f_{3\sigma'} c_{4\sigma} \\ &\quad + \frac{U_3}{2}\left(c^\dagger_{1\sigma} c^\dagger_{2\sigma'} f_{3\sigma'} f_{4\sigma} + \text{h.c.} \right) \end{aligned} \quad (11)$$

where $\sum_{[1234]}$ denotes the sum over all momenta subject to $\mathbf{k}_1 + \mathbf{k}_2 = \mathbf{k}_3 + \mathbf{k}_4$, and the summation over repeated spin indices is implied. Converting to new operators via Eq. (3) and keeping only the interactions which contribute to the pairing, we obtain from Eq. (11)

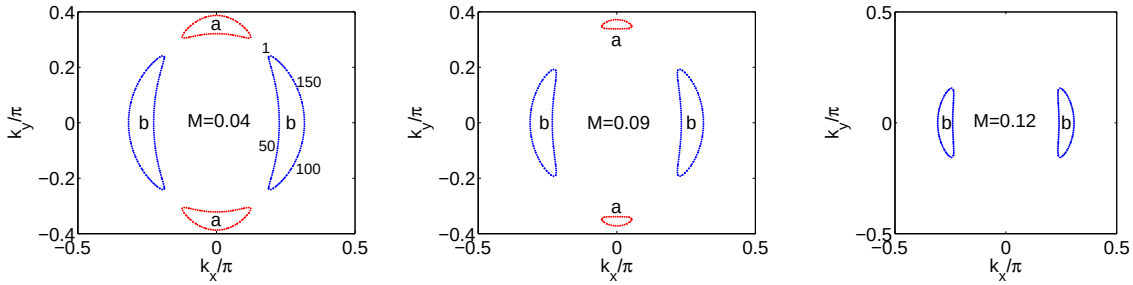

Figure 2: Reconstructed a and b Fermi pockets for several values of the SDW order parameter M. The a-pockets are smaller and disappear first upon increasing M. At even larger M, the b-pockets also disappear (not shown). Each pocket was discretized into a finite number of points indicated in the left figure for one of the b pockets. Our convention is such that the numbering for each pocket starts at the tip of a "banana" and goes first along the "inner" side of the pocket and then along the "outer" side.

$$H_{pair} = \sum_{\mathbf{q},\mathbf{k},\sigma,\sigma'} U^{aa}_{\mathbf{q},\mathbf{k}} \left(a^\dagger_{\mathbf{q}\sigma} a^\dagger_{-\mathbf{q}\sigma'} a_{-\mathbf{k}\sigma'} a_{\mathbf{k}\sigma} + b^\dagger_{\mathbf{q}\sigma} b^\dagger_{-\mathbf{q}\sigma'} b_{-\mathbf{k}\sigma'} b_{\mathbf{k}\sigma} \right) + \sum_{\mathbf{q},\mathbf{k},\sigma,\sigma'} U^{ab}_{\mathbf{q},\mathbf{k}} \left(a^\dagger_{\mathbf{q}\sigma} a^\dagger_{-\mathbf{q}\sigma'} b_{-\mathbf{k}\sigma} b_{\mathbf{k},\sigma} + \text{h.c.} \right) \quad (12)$$

where

$$U^{aa}_{\mathbf{q},\mathbf{k}} = U^{bb}_{\mathbf{q},\mathbf{k}} = \frac{U_3}{4} \left(-1 + \cos 2\theta_{\mathbf{q}} \cos 2\theta_{\mathbf{k}} + s \sin 2\theta_{\mathbf{q}} \sin 2\theta_{\mathbf{k}} \right)$$
$$U^{ab}_{\mathbf{q},\mathbf{k}} = U^{ba}_{\mathbf{q},\mathbf{k}} = -\frac{U_3}{4} \left(1 + \cos 2\theta_{\mathbf{q}} \cos 2\theta_{\mathbf{k}} + s \sin 2\theta_{\mathbf{q}} \sin 2\theta_{\mathbf{k}} \right)$$

and we defined $s \equiv U_1/U_3$.

We see from (12) that both intra-pocket and inter-pocket pairing interactions acquire angular dependence via the $\cos 2\theta_{\mathbf{q}}$, $\cos 2\theta_{\mathbf{k}}$ and $\sin 2\theta_{\mathbf{q}}$, $\sin 2\theta_{\mathbf{k}}$ factors. Constructing the set of linearized BCS gaps equations for the angle-dependent gaps $\Delta_a(\mathbf{q})$ and $\Delta_b(\mathbf{q})$ by standard means we find at $T = T_c$

$$\Delta_a(\mathbf{q}) = -\int_a \frac{dk_\parallel}{4\pi^2 v_F} U^{aa}_{\mathbf{q},\mathbf{k}} \Delta_a(\mathbf{k}) L - \int_b \frac{dk_\parallel}{4\pi^2 v_F} U^{ab}_{\mathbf{q},\mathbf{k}} \Delta_b(\mathbf{k}) L$$
$$\Delta_b(\mathbf{q}) = -\int_a \frac{dk_\parallel}{4\pi^2 v_F} U^{ba}_{\mathbf{q},\mathbf{k}} \Delta_a(\mathbf{k}) L - \int_b \frac{dk_\parallel}{4\pi^2 v_F} U^{bb}_{\mathbf{q},\mathbf{k}} \Delta_b(\mathbf{k}) L$$

where $L \equiv \log\left(\frac{\Lambda}{T_c}\right)$, Λ is the upper cutoff of the theory, and the Fermi velocity $v_F = v_F(k_\parallel)$ varies along $a-$and b Fermi surfaces.

A generic solution of this gap equation is of the form

$$\Delta_a(\mathbf{q}) = g_1 + g_2 \cos 2\theta_{\mathbf{q}} + g_3 \sin 2\theta_{\mathbf{q}}$$
$$\Delta_b(\mathbf{q}) = g_1 - g_2 \cos 2\theta_{\mathbf{q}} - g_3 \sin 2\theta_{\mathbf{q}} \quad (13)$$

Note, however, that the three angular components of $\Delta_{a,b}$ are not orthogonal, since e.g. $\int_a dq_\parallel \cos 2\theta_{\mathbf{q}}$ does not vanish. Substituting these expressions into the gap equation, we re-express it as a matrix equation for T_c and g_i:

$$\begin{pmatrix} g_1 \\ g_2 \\ g_3 \end{pmatrix} = \frac{U_3 L}{2} \begin{pmatrix} N & N_c & N_s \\ -N_c & -N_{cc} & -N_{cs} \\ -sN_s & -sN_{cs} & -sN_{ss} \end{pmatrix} \begin{pmatrix} g_1 \\ g_2 \\ g_3 \end{pmatrix} \quad (14)$$

where

$$N = 2\int_a \frac{dk_\parallel}{4\pi^2 v_F} + 2\int_b \frac{dk_\parallel}{4\pi^2 v_F}$$
$$N_c = 2\int_a \frac{dk_\parallel}{4\pi^2 v_F} \cos 2\theta_{\mathbf{k}} - 2\int_b \frac{dk_\parallel}{4\pi^2 v_F} \cos 2\theta_{\mathbf{k}}$$
$$N_s = 2\int_a \frac{dk_\parallel}{4\pi^2 v_F} \sin 2\theta_{\mathbf{k}} - 2\int_b \frac{dk_\parallel}{4\pi^2 v_F} \sin 2\theta_{\mathbf{k}}$$
$$N_{cc} = 2\int_a \frac{dk_\parallel}{4\pi^2 v_F} \cos^2 2\theta_{\mathbf{k}} + 2\int_b \frac{dk_\parallel}{4\pi^2 v_F} \cos^2 2\theta_{\mathbf{k}}$$
$$N_{ss} = 2\int_a \frac{dk_\parallel}{4\pi^2 v_F} \sin^2 2\theta_{\mathbf{k}} + 2\int_b \frac{dk_\parallel}{4\pi^2 v_F} \sin^2 2\theta_{\mathbf{k}}$$
$$N_{cs} = 2\int_a \frac{dk_\parallel}{4\pi^2 v_F} \cos 2\theta_{\mathbf{k}} \sin 2\theta_{\mathbf{k}} + 2\int_b \frac{dk_\parallel}{4\pi^2 v_F} \cos 2\theta_{\mathbf{k}} \sin 2\theta_{\mathbf{k}} \quad (15)$$

Without SDW order, $\sin 2\theta_k = 0$, $\cos 2\theta_k = \text{sign}(\epsilon_c - \epsilon_f)$, and N_s, N_{sc}, and N_{ss} all vanish. Then $g_3 = 0$, while $g_2/g_1 = -N_c/(N + \sqrt{N^2 - N_c^2})$. As a result, the gaps on the inner and outer sides of the a and b pockets reduce to $g_1(1 + N_c/(N + \sqrt{N^2 - N_c^2}))$ and $g_1(1 - N_c/(N + \sqrt{N^2 - N_c^2}))$. These two coincide with the gaps on the c and $f-$Fermi surfaces at T_c in the paramagnetic phase, which we set in our model to be angle-independent (we recall that the sign of the two gaps is the same because we attributed an extra minus sign to the gap on the $f-$Fermi surface by flipping the spins of $f-$fermions). The magnitudes of the gaps on c and

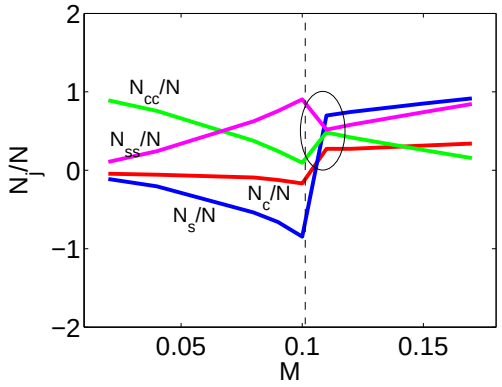

Figure 3: The quantities N_j/N, where $N_j = N_c, N_s, N_{cc}$, N_{ss}, plotted as functions of M. The dashed line indicates the value $M = M_1$ at which the a-pockets disappear. The ellipsis indicate the area around M_1 where the ratios rapidly evolve. Note that N_c/N remains small for all M, while N_s/N and N_{ss} increase with M and become positive and of order one at $M \geq M_1$.

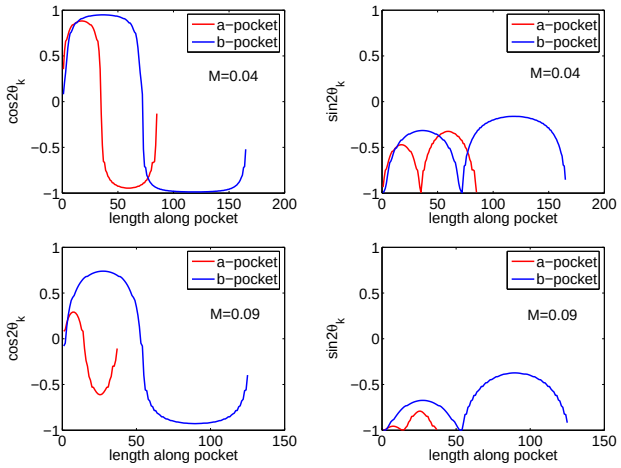

Figure 4: The behavior of $\cos 2\theta_{\mathbf{k}}$ (left column) and $\sin 2\theta_{\mathbf{k}}$ (right column) along the a and b pockets for $M = 0.04$ and $M = 0.09$. The gap is given by Eq. (13). The "length along the pocket" refers to the numbers along each pocket specified in Fig. 2.

$f-$ FSs are generally unequal as $N_c \neq 0$ because of the different geometry of hole and electron pockets. Numerically, however, for our set of parameters $N_c/N \ll 1$, i.e., at $M = 0$ the gaps on a and b FSs are essentially isotropic. Once SDW order sets in, all N_i and N_{ij} become non-zero, g_3 becomes finite, $\cos 2\theta_{\mathbf{k}}$ and $\sin 2\theta_{\mathbf{k}}$ become smooth functions along the pockets, and the gaps $\Delta_a(\mathbf{q})$ and $\Delta_b(\mathbf{q})$ acquire smooth angular variations. The magnitudes of the variations depend on the two parameters: the ratios g_2/g_1 and g_3/g_1 and the actual variation of $\cos 2\theta_{\mathbf{k}}$ and $\sin 2\theta_{\mathbf{k}}$ along $a-$and $b-$ Fermi surfaces.

In the small M limit, considered previously in Ref. 13, $\sin 2\theta_{\mathbf{k}}$ is small except for narrow ranges near the tips of the bananas. Then N_s, N_{sc}, and N_{ss} are small, and $N_{cc}/N \approx 1$. Solving Eq. (14) in this limit, we find that $g_3 \ll g_2 \ll g_1$, hence Δ_a and Δ_b remain almost constant along the $a-$ and $b-$pockets, including the tips of the bananas.

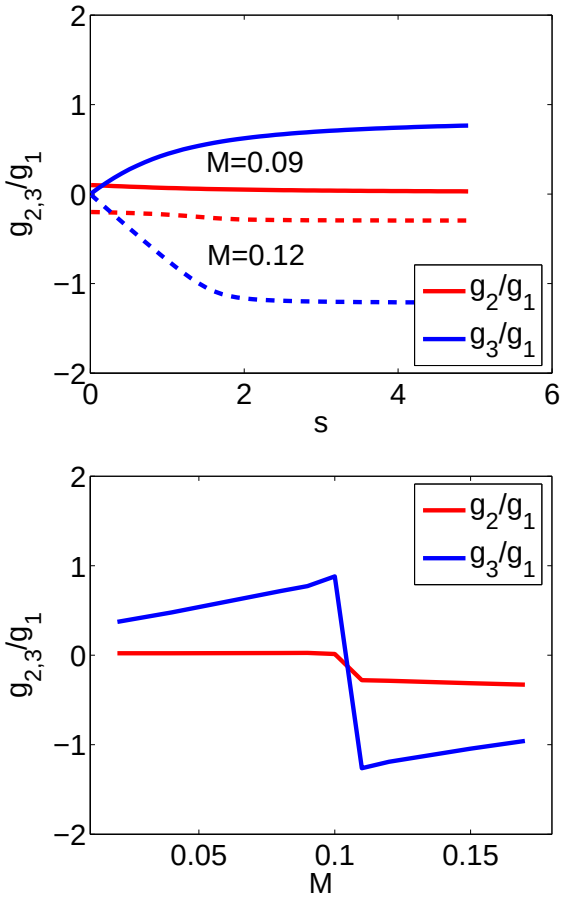

Figure 5: Top panel: the ratios g_2/g_1 (blue line) and g_3/g_1 (red line) as function of s for $M = 0.09$ (solid lines) and $M = 0.12$ (dashed lines). These values are slightly below and slightly above the critical $M_1 = 0.102$ at which two out of four pockets disappear. Both ratios flip sign between $M = 0.09$ and $M = 0.12$. The key result here is that for $s \geq 1$, the magnitude of g_3/g_1 becomes larger than 1 for $M = 0.12$. This gives rise to accidental nodes of the gap on the remaining FS pocket (see text). Bottom panel: the plot of the same ratios as functions of M for $s = 5$. The magnitude of g_2/g_1 remains relatively small, while the magnitude of g_3/g_1 becomes greater than 1 for $M \geq M_1$.

For arbitrary M, g_2/g_1 and g_3/g_1 are rather complex functions of the ratios N_j/N and also s. We plot N_j/N in Fig 3. We see that N_c/N and N_{cs}/N, are small because the integrands for N_c and N_{cs} contain $\cos 2\theta_k$, which changes sign between the inner and outer sides of the a and b-pockets (Fig. 4). At the same time, the magnitudes of N_s/N and N_{ss}/N increase with increasing M and become of order one.

In Fig. 4, we plot $\cos 2\theta_{\mathbf{k}}$ and $\sin 2\theta_{\mathbf{k}}$ along the a and

b-pockets. We recall that the prefactors of the $\cos 2\theta_{\mathbf{k}}$ terms in Δ_a and Δ_b are already small because g_2/g_1 is small. Fig. 4 shows that the variation of $\cos 2\theta_{\mathbf{k}}$ along each of the pockets decreases with increasing M, making the $g_2 \cos 2\theta_{\mathbf{k}}$ term even less relevant. On the other hand, the range where $|\sin 2\theta_{\mathbf{k}}|$ is not small widens up with increasing M. Over some range of M, up to $M_{11} = 0.5(m_y - m)/(m_y + m) < M_1$ on the a-pocket and up to $M_{22} = 0.5(m - m_x)/(m + m_x) < M_2$ on the b-pocket, $\sin 2\theta_{\mathbf{k}}$ varies between -1 and some negative value. At $M_{11} < M < M_1$, $\sin 2\theta_{\mathbf{k}}$ on the a-pocket varies in a more narrow interval, does not reach -1 and eventually becomes

$$\sin 2\theta_{\mathbf{k}_a\, M \to M_1} = -2\frac{\sqrt{m m_y}}{m + m_y} = -0.98. \qquad (16)$$

The same behavior holds for $\sin 2\theta_{\mathbf{k}}$ on the $b-$pocket for $M_{22} < M < M_2$, but with

$$\sin 2\theta_{\mathbf{k}_b\, M \to M_2} = -2\frac{\sqrt{m m_x}}{m + m_x} = -0.94. \qquad (17)$$

III. GAP STRUCTURE IN THE COEXISTENCE STATE AS FUNCTION OF M

A. From small to intermediate M: nodeless-nodal transition

We now discuss in more detail the solution of the matrix equation (14) and the structure of the SC gap. We found in the previous section that the angular dependence of $\cos 2\theta_{\mathbf{k}}$ and $\sin 2\theta_{\mathbf{k}}$ along the a and $b-$ pockets depends on M, while the solution of the matrix equation for g_i depends on M and also on s - which, we remind, is the ratio of the interactions $s = U_1/U_3$.

The solution of the matrix equation can be easily analyzed in the limits of small and large s. At small s, g_3 is small compared to g_2 ($g_3/g_2 = O(s)$), while g_2/g_1 is given by

$$\frac{g_2}{g_1} \approx -\frac{N_c}{N + N_{cc}} \qquad (18)$$

This ratio is always small because N_c/N is small for all M (see Fig. 3). As a result, the gaps $\Delta_a(q)$ and $\Delta_b(q)$ remain essentially constants regardless of how strong the SDW order is.

In the opposite limit $s \gg 1$ the behavior is different. Only in a narrow range of the smallest $M \ll 1/s$ the gaps remain almost angle-independent. Outside this range g_2 is small compared to g_3 ($g_2/g_3 = O(1/s)$), while g_3/g_1 is given by

$$\frac{g_3}{g_1} \approx -\frac{N_s}{N_{ss}} \qquad (19)$$

Both N_s and N_{ss} become non-zero at a finite M and their ratio is of order one, i.e., $g_3 \sim g_1$. This leads to sizable angular dependencies of $\Delta_a(q)$ and $\Delta_b(q)$. For small $M < M_1$, N_s is smaller in magnitude than N_{ss} (see Fig. 3), hence $|\frac{g_3}{g_1}| < 1$ and the angular variations of the gaps do not give rise to nodes. However, as M increases and approaches M_1, the ratio N_s/N_{ss} changes sign, becomes negative and its magnitude exceeds one (see Fig. 3). The combination of this behavior and the fact that for $M \sim M_1$ $\sin 2\theta$ reaches -1 at the tip of the bananas implies that the gap along the $b-$ pocket develops accidental nodes. This happens even before M reaches M_1 because at $M = M_1$ (when the $a-$pocket disappears), $|N_s/N_{ss}|$ is already larger than one, as one can immediately see from Eq. 15, if one neglects in this equation the contributions from the a pocket. The nodes in $\Delta_b(\mathbf{q})$ obviously survive up to M_{22} because at $M < M_{22}$ the minimal value of $\sin 2\theta_{\mathbf{q}}$ remains -1. At larger $M_{22} < M < M_2$ this minimal value becomes smaller than one, but we checked numerically that the nodes still survive and remain present up to $M = M_2$.

To understand the gap structure in between the limits $s \ll 1$ and $s \gg 1$, we solve the 3×3 gap equation (14) numerically for several s with M as a running parameter, and for several M with s as a running parameter. In the two panels in Fig. 5 we plot the ratios g_2/g_1 and g_3/g_1 as function of s for two representative values of M, $M = 0.09 < M_1$ and $M_1 < M = 0.12 < M_2$, and as function of M for $s = 5$. We see that $|g_2/g_1|$ is always small, while $|g_3/g_1|$ increases with increasing s and for $M = 0.12$ becomes larger than 1 above a certain s. Once this happens, the gap on the $b-$pocket develops accidental nodes. Overall, these results show that the behavior that we obtained analytically at large s extends to all $s \geq 1$. For these values of s, the gap along the $b-$pocket, which survives up to larger M, necessarily develops accidental nodes around $M = M_1$, where the a-pocket disappears.

In Fig. 6 we show the variations of $\Delta_a(\mathbf{q})$ and $\Delta_b(\mathbf{q})$ for two different values of s, $s = 1$ and $s = 5$, and three different values of M: $M \ll M_1$, $M \leq M_1$, and $M_1 < M < M_2$. For $s = 1$, the gaps Δ_a and Δ_b have no nodes for all M, consistent with $|g_3/g_1| < 1$ in Fig. 5. The only effect of the disappearance of the $a-$pockets is the switch between the maxima and the minima of the gap function along the remaining b-pockets. This switch is a consequence of the sign change of both g_2/g_1 and g_3/g_1 (see Fig. 5).

The situation is different for larger $s = 5$. Even for small $M \ll M_1$, the gap variation along both $a-$and $b-$pockets become substantial. Once M becomes large enough to (almost) gap out the a-pockets, the nodes appear near the tips of the $b-$pocket bananas. This behavior is in full agreement with the analysis of g_3/g_1 earlier in this section.

We therefore conclude that the two conditions to obtain nodes in the superconducting gap in the coexistence phase with stripe antiferromagnetism are: (i) relatively large density-density interaction U_1 (leading to

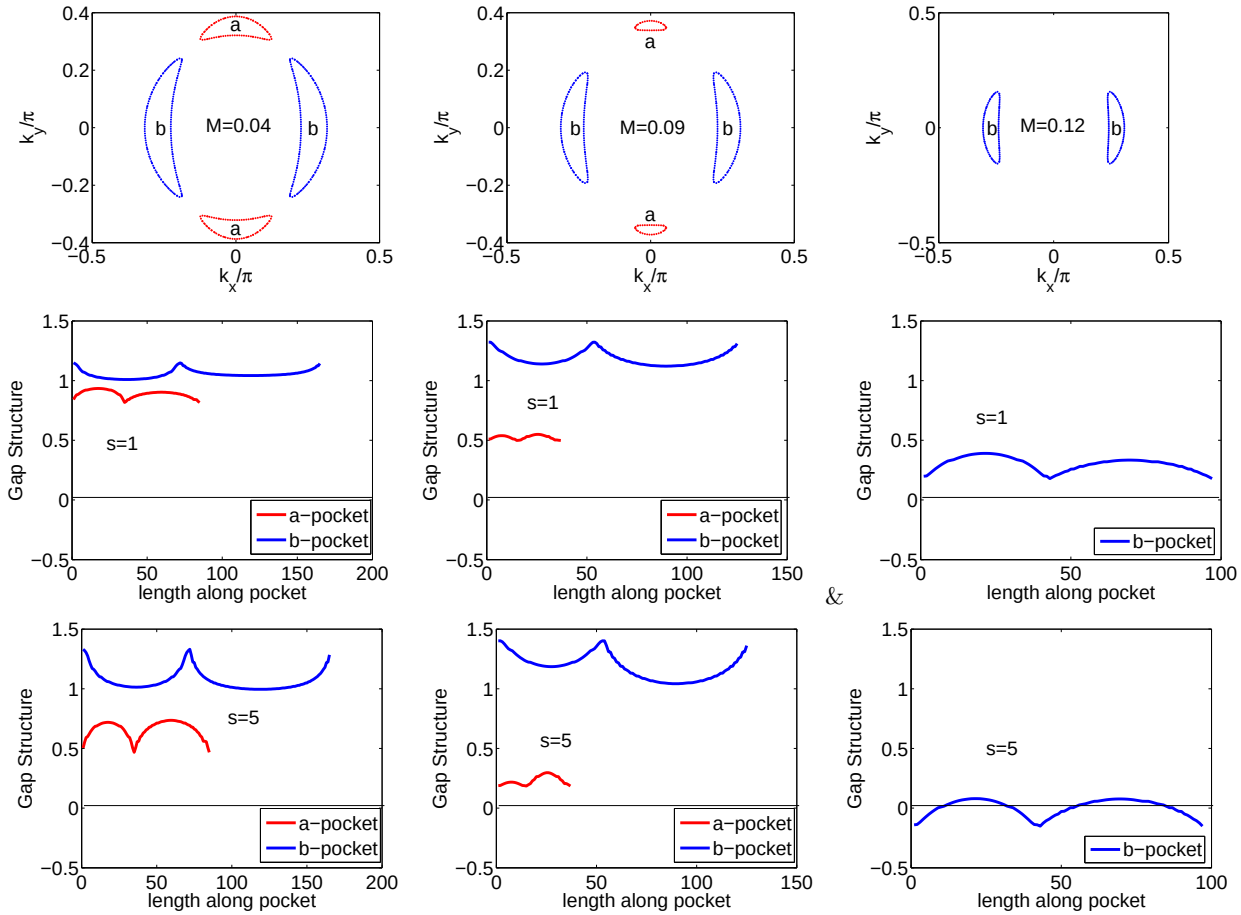

Figure 6: The gap structure for two values of $s = U_1/U_3$ and three different M corresponding to the cases when the a and b-pockets are of comparable size (left column), when the a pockets are about to disappear (middle column), and when only the $b-$pockets are left (right column). Note the appearance of gap nodes for $s = 5$ and $M = 0.12$, when one pair of reconstructed pockets disappear.

magnetism) compared to the pair-hopping interaction U_3, and (ii) the disappearance of one of the two pairs of reconstructed Fermi pockets. Our analysis agrees with previous works that found fully gapped quasi-particle excitations in the coexistence state in the cases of small M (Ref. 13) and $U_1 = 0$ (Ref. 15).

The other interactions, which we listed in Sec. II but did not include into H_{int} in Eq. (11), modify the value of s and therefore affect whether or not the nodes appear upon increasing M. In particular, the exchange term $\left[U_2 c^\dagger_\sigma f_\sigma f^\dagger_{\sigma'} c_{\sigma'}\right]$ changes s to $s = \frac{U_1 - U_2}{U_3}$. If U_2 is negative, it makes the development of nodes more likely, while if it is positive and smaller than U_1, it decreases s and may eliminate the nodes. The inclusion of this term also opens up the somewhat exotic possibility of a negative s. Although negative s is unlikely for FeSCs, we analyzed the $s < 0$ case for completeness and show the results in Fig. 7. We see that now the behavior is non-monotonic with s: the nodes appear at some intermediate $|s|$ and disappear at larger $|s|$, already at relatively small M, when all four pockets are present.

B. From intermediate to large M: nodal-nodeless transition

In the previous section we showed that nodes appear at large enough s at intermediate values of $M \sim M_1$, where one of the two pairs of reconstructed pockets (the a-pocket) disappears. We now analyze what happens when M becomes larger than M_2 and b-pockets also disappear.

We find that the results depend on whether we restrict the pairing to the FS or include into the pairing problem also the states which are already gapped out by SDW. If we restrict the pairing problem to the FS, as we did before, we find that the nodes in Δ_b are present for all $M < M_2$. At $M = M_2$ the remaining FS disappears and T_c vanishes. If we do not restrict the pairing to the FS and take into consideration the states already gapped by SDW, SC persists into the region $M > M_2$ (see Refs. 14,16,24). In this last region, all states are gapped already above T_c, and the opening of an additional SC gap only moves states further away from zero energy.

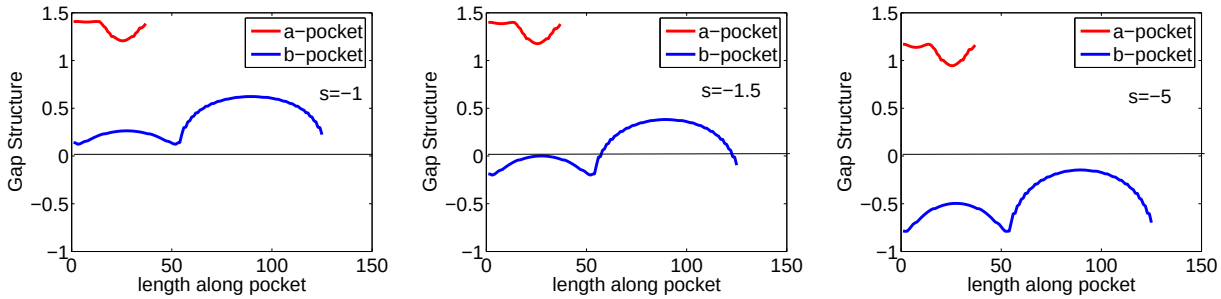

Figure 7: Gap structure for negative s and $M = 0.09$. As $|s|$ increases, the gap on the b pocket is pushed down, acquires the nodes, and eventually reverses sign and again becomes nodeless. For all three values of s the FS contains both a and b pockets.

The thermal conductivity and the penetration depth in this last regime show exponential behavior, typical for a superconductor with a full gap, From this perspective, the evolution of the system response around $M = M_2$ mimics the transformation from a nodal to a nodeless gap, irrespective of whether the actual SC gap by itself evolves around M_2.

On a more careful look, we find that the gap Δ_b does change its structure near $M = M_2$ and becomes nodeless. At around the same M, T_c is likely non-monotonic and passes through a minimum.

The argument goes as follows. Consider first the pairing confined to the FS and solve for T_c. Neglecting N_c and N_{cs} in Eq. (14), which are small for all M and s, and solving for the linearized gap equation for $L = \log\left(\frac{\Lambda}{T_c}\right)$, we obtain

$$1 + \frac{U_3}{2}\left(sN_{ss} - N\right)L + \left(\frac{U_3}{2}\right)^2 s\left(N_s^2 - NN_{ss}\right)L^2 = 0 \tag{20}$$

One can verify that $NN_{ss} - N_s^2$ is positive for all $M > M_2$. For $s \geq 1$, when Δ_b has nodes at $M \sim M_1$, we also have $sN_{ss} > N$. In this situation, there is a single solution of (20) with $L > 0$:

$$L = \frac{1}{sU_3(NN_{ss} - N_s^2)} \times \left(\sqrt{(sN_{ss} + N)^2 - 4sN_s^2} + (sN_{ss} - N)\right) \tag{21}$$

As long as $N_s^2 \ll NN_{ss}$, $L \approx 2/U_3N$, i.e. T_c does not depend strongly on M. However, near $M = M_2$, $\sin 2\theta(\mathbf{k})$ on the $b-$pockets tends to a constant value c, see Eq. (17), ($c = -0.94$ for our parameters) and N_s^2 and NN_{ss} both tend to the same value c^2N^2. As a result, L diverges as $(2/U_3s)(sN_{ss} - N)/(NN_{ss} - N_s^2)$, i.e. T_c vanishes (see Fig 8). One can straightforwardly show that L diverges at $M = M_2$ even if we solve the full 3×3 linearized matrix gap equation, without neglecting the terms N_c and N_{cs}.

In the same limit $NN_{ss} \approx N_s^2$, we also have

$$\frac{g_3}{g_1}\sin 2\theta_{\mathbf{q}} = -\frac{N_s}{N_{ss}}\sin 2\theta_{\mathbf{q}} \to -c\frac{-c}{c^2} = 1. \tag{22}$$

We see that the angle-independent and the $\sin 2\theta$ terms in Δ_b become identical and cancel each other, i.e Δ_b vanishes (see Eq. (13)). This is consistent with the vanishing of T_c.

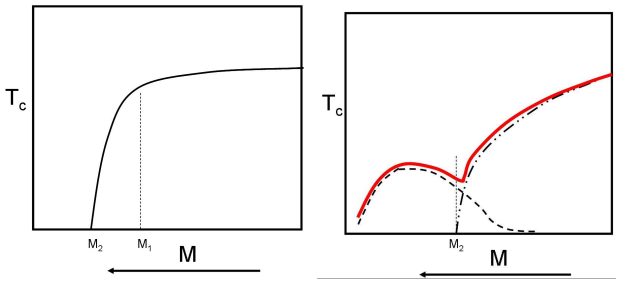

Figure 8: a) Schematic behavior of T_c as a function of M, if T_c is obtained by restricting to contributions only from the FSs. This T_c drops to zero as $M \to M_2$. The arrow indicates the direction along which M increases. b) The actual T_c (solid red line) is a superposition of contributions from the FS and from the gapped states (dashed lines). This T_c initially decreases when M approaches M_2 but reverses the trend and remains finite at M_2 and even in some range of $M > M_2$. The dip in T_c is in the region where the contributions from the FS and from the gapped states become comparable to each other. This non-monotonic behavior of T_c around M_2 is captured by Eq. (24) (see text).

These results, however, hold only as long as we restrict the integrals for N, N_s, and N_{ss} to the FS. Once we include the contributions from the gapped states, N_s^2 and NN_{ss} no longer tend to the same value. The contributions from the gapped states contain, instead of $L = \log\Lambda/T_c$, the factor $L_D = \log\Lambda/\sqrt{D^2 + T_c^2}$, where D is the gap in the absence of SC. In a generic weak coupling case, these contributions would be small in L_D/L compared to the contributions from the FS, but in our case the FS contribution to $NN_{ss} - N_s^2$ vanishes at M_2, and the contribution from the gapped states become the dominant ones. Similarly, contributions from the gapped state break the cancelation between the angle-independent and the $\sin 2\theta_{\mathbf{q}}$ terms in Δ_b.

Combining the contributions from the FS and from the

gapped states to N_i, we have near $M = M_2$,

$$\begin{aligned} N &= N_0\left(1+\gamma\frac{L_D}{L}\right) \\ N_s &= N_0\left(c_s-\gamma_s\frac{L_D}{L}\right) \\ N_{ss} &= N_0\left(c_{ss}+\gamma_{ss}\frac{L_D}{L}\right) \end{aligned} \tag{23}$$

where $c_s \approx -c > 0$ and $c_{ss} \approx c^2$. One can introduce $\epsilon \equiv c_{ss} - c_s^2$ as a measure of deviation from M_2, with $\epsilon = 0$ at M_2. The constants γ_i are all positive, at least if they predominantly come from gapped $a-$pockets. Since $\sin 2\theta_{\mathbf{q}}$ along the $a-$pockets is quite close to -1 (see Fig. 4), we have $\gamma_s^2 = \gamma\gamma_{ss}$ to a good accuracy. Substituting these forms into the result for L, Eq. (21), and assuming for simplicity that $s \gg 1$, we obtain for small ϵ

$$\begin{aligned} &\epsilon\tilde{L}^2 + K_1\tilde{L} - K_2 = 0 \\ &K_1 = \left(\gamma c^2 + \gamma_{ss} + 2\gamma_s|c|\right)\tilde{L}_D - c^2 \\ &K_2 = \gamma_{ss}\tilde{L}_D > 0 \end{aligned} \tag{24}$$

where $\tilde{L} = L(N_0U_3/2)$, $\tilde{L}_D = L_D(N_0U_3/2)$. If we set $\tilde{L}_D = 0$, i.e., neglect the contributions from the gapped states, $K_2 = 0$, $K_1 = -c^2$, and we obtain $\tilde{L} = c^2/\epsilon$, as before. If instead we set $\epsilon = 0$, we find that L remains finite and positive, and to leading order in $\tilde{L}_D^{-1} < 1$ is given by

$$\tilde{L}_{\epsilon=0} \approx \frac{\gamma_{ss}}{\gamma_{ss} + \gamma c^2 + 2\gamma_s|c|} \tag{25}$$

The behavior of $\tilde{L}$ at small but finite ϵ is rather involved, but its main features can be understood directly from Eq. (24). Far from M_2, T_c is not small, implying that $\tilde{L}_D$ is small, i.e and $K_1 < 0$ and K_2 can be neglected. As a result, $\tilde{L}$ increases as $\tilde{L} \sim 1/\epsilon$, leading to a decrease in T_c and, consequently, to an increase in $\tilde{L}_D$. With increasing $\tilde{L}_D$, K_1 crosses zero and changes sign. At this point, $K_2 = \mathcal{O}(1)$, and $\tilde{L} \sim K_2/\sqrt{\epsilon} \sim 1/\sqrt{\epsilon}$, i.e., it still increases with decreasing ϵ, but more slowly then before. Because $\tilde{L}_{\epsilon=0} \sim \mathcal{O}(1)$ given by (25) is certainly smaller than $1/\sqrt{\epsilon}$, $\tilde{L}$ necessary passes through a maximum near the point where K_1 changes sign, and then decreases towards $\tilde{L}_{\epsilon=0}$. Accordingly, $T_c = \Lambda e^{-2\tilde{L}/U_3N_0}$ passes through a minimum at some $M \leq M_2$, as shown schematically in Fig. 8

Contributions from the gapped states also affect the interplay between the constant and the $\sin 2\theta_{\mathbf{q}}$ terms in Δ_b. if we include these terms, we obtain, near $M = M_2$, instead of Eq. (22),

$$\frac{g_3}{g_1}\sin 2\theta_{\mathbf{q}} = \frac{1+\frac{\gamma_s}{c}\frac{L_D}{L}}{1+\frac{\gamma_{ss}}{c^2}\frac{L_D}{L}} \tag{26}$$

where, we remind, in our case $\gamma_{s,ss} > 0$ and $c = -0.94$. We see that the numerator gets smaller than one and the denominator gets larger than one. As a result, $|\frac{g_3}{g_1}\sin 2\theta_{\mathbf{q}}|$ becomes smaller than one, and the gap Δ_b recovers its nodeless form in the vicinity of M_2. Very likely Δ_b remains gapless also at larger M, before T_c finally vanishes.

We also note that our consideration is self-consistent in the sense that the transformation from nodal to nodeless gap and non-vanishing of T_c at $M = M_2$, where $\epsilon = 0$, are consistent with each other. Indeed, once the gap Δ_b becomes nodeless, the pairing problem at $M \geq M_2$ is qualitatively similar to the one for fermions with the dispersion

$$\varepsilon_{gapped}(k) = \sqrt{D^2 + \left[\mathbf{v}_F\cdot(\mathbf{k}-\mathbf{k}_F)\right]^2}, \tag{27}$$

where D is the pre-existing gap in the excitation spectrum. For such model, T_c is non-zero at $D = 0$ (equivalent of $M = M_2$) and extends into the region where $D \neq 0$:

$$T_c(D) = T_c(0)F\left[\frac{D}{T_c(0)}\right] \tag{28}$$

where $F(x)$ is a decreasing function of x subject to $F(x \to 0) = 1 - x^2$ and $F(x) = -1/\ln(1.76 - x)$ near the critical $x = 1.76$.

The outcome of this analysis is that nodal SC gap exists only in relatively narrow range of M, from $M \leq M_1$ to $M \leq M_2$. At larger M the gap is again nodeless, and, furthermore, for $M > M_2$ all low-energy states are gapped already above T_c. The SC transition temperature T_c is non-zero at M_2 and decreases into $M > M_2$ region. Before that, T_c has a minimum roughly where the gap changes from nodal to nodeless.

C. Role of the non-reconstructed pockets

So far, we have restricted our consideration of the pairing problem to one hole and one electron pocket reconstructed by SDW. There are additional pockets which do not participate in the SDW state[17]. In this subsection we analyze to what extent these additional pockets affect our results. Specifically, we add another elliptical electron pocket centered at $(\pi, 0)$, denote fermions near this pocket by $d_{\mathbf{k}}$, and solve the set of coupled linearized gap equations for $\Delta_a(\mathbf{q})$, $\Delta_b(\mathbf{q})$, and $\Delta_d(\mathbf{q})$. The interactions involving fermions near $(0, 0)$ and near the electron pocket at $(\pi, 0)$ are the same as the interactions between $(0, 0)$ and $(0, \pi)$, i.e., the couplings are the same U_1, U_2, U_3, and U_4. As before, we consider the model with only U_3 and $U_1 = sU_3$. We also neglect direct interaction between electron pockets.

The effective pairing interactions in the $a-b-d$ space are obtained by dressing the interactions by coherence factors associated with the transformation from c and f to a and b operators for the pockets at $(0, 0)$ and at $(0, \pi)$. Since the expressions for the vertices are long, we

refrain from presenting them. Yet, it is straightforward to obtain and solve the set of linearized gap equations for $\Delta_a(\mathbf{q})$, $\Delta_b(\mathbf{q})$, and $\Delta_d(\mathbf{q})$. It is essential that the "dressing" does not involve $d-$fermions, hence the interaction has no dependence on the angle along the $d-$FS. As a consequence, $\Delta_d(\mathbf{q})$ remains angle-independent. This constant Δ_d, however, affects the interplay between the angle-independent and the $\cos 2\theta_{\mathbf{k}}$ and $\sin 2\theta_{\mathbf{k}}$ terms for $\Delta_a(\mathbf{q})$ and $\Delta_b(\mathbf{q})$.

In Fig. 9, we show the gap structure obtained from the solution of the pairing problem for $s = 5$ and the same three values of M as in Fig. 6. Comparing Figs. 6 and Fig. 9, we see that the non-reconstructed d-pocket has only a minor effect on the $a - b$ gap structure – the gap on the b pocket still becomes more angle-dependent with increasing M and develops accidental nodes at $M \geq M_1$. In view of this result, it is very likely that the physics of gap variation with M is fully captured already within the two-band model of one hole and one electron pocket.

IV. EFFECT OF AN EXTERNAL MAGNETIC FIELD

We now consider how the SC gap structure is affected by an external magnetic field $\mathbf{H}$. The specific goal is to verify whether the field increases or reduces the tendency towards the development of nodes in Δ_b. This issue is related to experiments on $(Ba_{1-x}K_x)Fe_2As_2$, particularly to recent measurements of thermal conductivity in a field[22].

We direct the field along z and include into the Hamiltonian the Zeeman coupling between the field and the $z-$component of the spin of a fermion $S_z = (1/2)c^\dagger_\alpha \sigma^z_{\alpha\beta} c_\beta$. For an isotropic system, the SDW vector $\mathbf{M}$ is oriented transverse to $\mathbf{H}$ and for definiteness we direct it along x. At a finite H, the system also develops a non-zero uniform magnetization, which rotates a spin at a given site towards the field and creates a canted two-sublattice structure, with orthogonal antiferromagnetic SDW component $\mathbf{M} = M_x$ and ferromagnetic component along z.

The quadratic part of the Hamiltonian in the presence of the field is

$$\begin{aligned} H &= \sum_{\mathbf{k},\sigma} \left[(\varepsilon^c_{\mathbf{k}} + \sigma h)\, c^\dagger_{\mathbf{k}\sigma} c_{\mathbf{k}\sigma} + \left(\varepsilon^f_{\mathbf{k}+\mathbf{Q}} + \sigma h\right) f^\dagger_{\mathbf{k}+\mathbf{Q}\sigma} f_{\mathbf{k}+\mathbf{Q}\sigma} \right] \\ &+ \sum_{\mathbf{k}} M \left(c^\dagger_{\mathbf{k}\uparrow} f_{\mathbf{k}+\mathbf{Q}\downarrow} + c^\dagger_{\mathbf{k}\downarrow} f_{\mathbf{k}+\mathbf{Q}\uparrow} + \text{h.c.} \right) \end{aligned} \tag{29}$$

where $h = \mu_B H$. We will measure h in units of 2μ, as with other observables.

The transformation to the new operators is now given by

$$\begin{pmatrix} \sigma a_{\mathbf{k}\sigma} \\ b_{\mathbf{k}\sigma} \end{pmatrix} = \begin{pmatrix} -\sigma \cos\theta_{\mathbf{k},\sigma} & \sin\theta_{\mathbf{k},\sigma} \\ -\sin\theta_{\mathbf{k},\sigma} & -\sigma\cos\theta_{\mathbf{k},\sigma} \end{pmatrix} \begin{pmatrix} c_{\mathbf{k}\sigma} \\ f_{\mathbf{k}+\mathbf{Q}\sigma} \end{pmatrix} \tag{30}$$

where

$$\begin{aligned} \cos\theta_{\mathbf{k},\sigma} &= \frac{M}{\sqrt{M^2 + (E^-_\sigma)^2}} \\ \sin\theta_{\mathbf{k},\sigma} &= \frac{E^-_\sigma}{\sqrt{M^2 + (E^-_\sigma)^2}} \end{aligned} \tag{31}$$

and

$$E^-_\sigma = \left(\frac{\varepsilon^c - \varepsilon^f}{2} + \sigma h\right) - \sqrt{\left(\frac{\varepsilon^c - \varepsilon^f}{2} + \sigma h\right)^2 + M^2} \tag{32}$$

Substituting the transformation into H_{int} in Eq. (11) and taking care of the fact that $\cos\theta_{k,\uparrow}$ and $\cos\theta_{k,\downarrow}$ are now different, we obtain Eq. (12) but with new $U^{aa}_{\mathbf{q},\mathbf{k}}$, $U^{bb}_{\mathbf{q},\mathbf{k}}$ and $U^{ab}_{\mathbf{q},\mathbf{k}}$ given by

$$\begin{aligned} U^{aa}_{\mathbf{q},\mathbf{k}} &= U^{bb}_{\mathbf{q},\mathbf{k}} = -\frac{U_3}{2}\left(C_{\mathbf{q}\uparrow}C_{-\mathbf{q}\downarrow}S_{\mathbf{k}\uparrow}S_{-\mathbf{k}\downarrow} + S_{\mathbf{q}\uparrow}S_{-\mathbf{q}\downarrow}C_{\mathbf{k}\uparrow}C_{-\mathbf{k}\downarrow}\right) + U_1 C_{\mathbf{q}\uparrow}S_{-\mathbf{q}\downarrow}C_{\mathbf{k}\uparrow}S_{-\mathbf{k}\downarrow} \\ U^{ab}_{\mathbf{q},\mathbf{k}} &= U^{ba}_{\mathbf{q},\mathbf{k}} = -\frac{U_3}{2}\left(C_{\mathbf{q}\uparrow}C_{-\mathbf{q}\downarrow}C_{\mathbf{k}\uparrow}C_{-\mathbf{k}\downarrow} + S_{\mathbf{q}\uparrow}S_{-\mathbf{q}\downarrow}S_{\mathbf{k}\uparrow}S_{-\mathbf{k}\downarrow}\right) - U_1 C_{\mathbf{q}\uparrow}S_{-\mathbf{q}\downarrow}C_{\mathbf{k}\uparrow}S_{-\mathbf{k}\downarrow} \end{aligned}$$

where $C_{\mathbf{k},\sigma} \equiv \cos\theta_{\mathbf{k},\sigma}$ and $S_{\mathbf{k},\sigma} \equiv \sin\theta_{\mathbf{k},\sigma}$. The gap structure consistent with these $U^{ij}_{\mathbf{q},\mathbf{k}}$ is of the form

$$\begin{aligned} \Delta_a(\mathbf{q}) &= g_1 C_{\mathbf{q}\uparrow}C_{-\mathbf{q}\downarrow} + g_2 S_{\mathbf{q}\uparrow}S_{-\mathbf{q}\downarrow} \\ &\quad + g_3 C_{\mathbf{q}\uparrow}S_{-\mathbf{q}\downarrow} + g_4 S_{\mathbf{q}\uparrow}C_{-\mathbf{q}\downarrow} \\ \Delta_b(\mathbf{q}) &= g_1 C_{\mathbf{q}\uparrow}C_{-\mathbf{q}\downarrow} + g_2 S_{\mathbf{q}\uparrow}S_{-\mathbf{q}\downarrow} \\ &\quad - g_3 C_{\mathbf{q}\uparrow}S_{-\mathbf{q}\downarrow} - g_4 S_{\mathbf{q}\uparrow}C_{-\mathbf{q}\downarrow} \end{aligned}$$

We constructed the set of coupled linearized gap equations for g_i by standard means and solved them for various M, $s = U_1/U_3$ and h. We found that the field enhances the angle variation of the gaps Δ_a and Δ_b, such that nodes appear at smaller M and smaller s. To illustrate this, in Fig. 10 we compare the gap structure for a given $M = 0.04$ and $s = 1$ (same as in the upper left panel in Fig. 6) without a field and with a field. We clearly see that the gap variations along the reconstructed FSs grow with the field, and for large enough field nodes appear

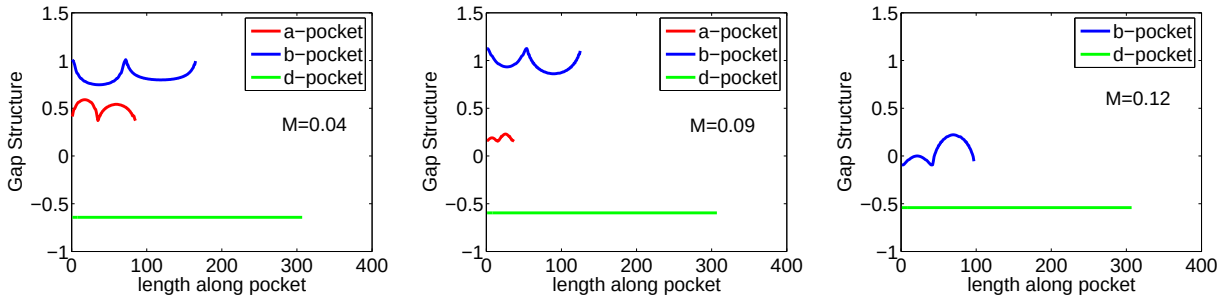

Figure 9: The gap structure for $s = 5$ and the same values of M as used in Fig. 6 for the case when we include an additional, spectator pocket at $(\pi, 0)$ which does not participate in the FS reconstruction. A comparison with Fig. 6 shows that the gap structure is almost unaffected by the presence of the spectator pocket.

well before M reaches the value at which the $a-$pockets disappear. The implication is that the range where the gap has nodes widens up with the application of a field and, in particular, extends to smaller M (larger dopings), where without a field the system was a superconductor with a nodeless gap.

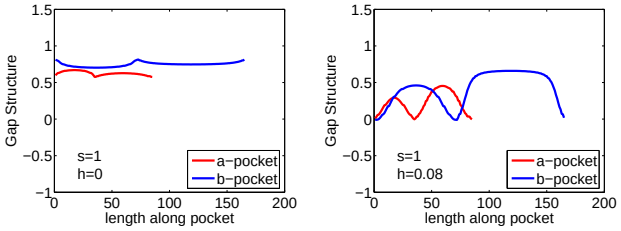

Figure 10: The gap structure for $h = 0$ (left panel) and $h = 0.08$ (right panel) for $M = 0.04$ and $s = 1$. The application of the field increases angle variations of the gaps and leads to the appearance of nodes at a smaller M (and a smaller s) than without a field.

We emphasize that the extension of the nodal region to smaller M is a different effect than the field-induced changes in M_1 and M_2. These last changes are due to the modification of the quasiparticle dispersion, which in the presence of the field becomes 4-band dispersions and takes the form

$$E^{a,b}_{\mathbf{k}} = \frac{\varepsilon^c + \varepsilon^f}{2} \pm \sqrt{\left(\frac{\varepsilon^c - \varepsilon^f}{2} \pm h\right)^2 + M^2} \qquad (33)$$

The two a-pockets are split by $\pm h$ into a^+ and a^- pockets, and the two $b-$pockets are split by $\pm h$ into b^+ and b^- pockets.

The presence of $\pm h$ under the square root splits M_1 and M_2 into M_1^+, M_1^- and M_2^+, M_2^-, where $M_{1,2}^+ = M_{1,2}(1 + 2h)$ and $M_{1,2}^- = M_{1,2}(1 - 2h)$, with M_1 and M_2 given by Eqs 9 and 10 (we recall that h is measured in units of 2μ). For $h = 0.08$ used in Fig. 10 we get $M_1^+ = 0.118$, $M_1^- = 0.086$ instead of $M_1 = 0.102$, and $M_2^+ = 0.205$, $M_2^- = 0.149$ instead of $M_2 = 0.177$. Clearly, the field-induced changes in the form of reconstructed FSs are small compared to the changes of the SC gap structure associated with the field-induced change of the pairing interaction. The small effect of the field on the reconstructed FS is in agreement with previous works on the cuprates[25].

V. DISCUSSION AND CONCLUDING REMARKS

We showed that the superconducting gap of an s^{+-} SC in the co-existence phase with an SDW order acquires additional angular dependence compared to the case when SDW order is not present. In particular, an isotropic pairing interaction becomes angle-dependent inside the SDW state. At small SDW order parameter M, or when the density-density interaction between the hole and electron pockets is small compared to pair hopping interaction term, this extra dependence is weak, in agreement with previous studies[13,15]. However, when density-density and pair hopping interactions are comparable and M is large enough to gap out one out of two pairs of reconstructed FS pockets, the angular dependence gets quite strong and the SC gap on the remaining FS banana-like pocket develops accidental nodes near the tips of the bananas. At even larger M, the system bounces back into the fully gapped SC state which extends into the regime where large enough M gaps out the remaining pair of FS pockets. The SC transition temperature T_c has a dip near the point where nodal SC state becomes nodeless. In the presence of a magnetic field, the width of the nodal region expands, and, in particular, the nodes appear at smaller M (larger doping).

Our results offer a consistent explanation for the recent experimental observations[22] in underdoped $(Ba_{1-x}K_x)Fe_2As_2$. Performing in-plane thermal conductivity measurements, Reid *et al.* found a small range of doping in the SC-SDW coexistence region where the ratio κ/T is finite at $T = 0$, i.e., κ is linear in T at small T. This linearity is generally viewed as a strong indication for the presence of the nodes in the SC gap. At smaller and larger dopings Reid *et al.* found that κ/T vanishes at $T = 0$, as it is expected for a fully gapped supercon-

ductor. They also observed that the doping range where κ/T is finite at $T = 0$ expands upon the application of an external magnetic field.

In terms of our model, the nodeless-nodal-nodeless transition observed by Reid *et al.* can be attributed to the following sequence of events: at the optimal doping, which roughly coincides with the onset of the co-existence range, the SC gaps in $(Ba_{1-x}K_x)Fe_2As_2$ are almost isotropic, and the excitation spectrum is fully gapped. Decreasing x and moving to the underdoped region in which SC and SDW start to coexist is equivalent to making M nonzero in our model. In this situation, the gaps become anisotropic, but remain nodeless over some range of M. Moving deeper inside the coexistence region is equivalent to making M larger. Eventually, M becomes large enough such that one of the reconstructed pairs of pockets vanishes. In this situation, we found (for $s \geq 1$) that the gap on the remaining FS pockets develops nodes, what leads to a finite κ/T at $T = 0$. As the doping level decreases even further, M continues to increase and the gap structure bounces back to nodeless, since for such pairing state T_c remains non-zero even when the remaining pair of reconstructed pockets disappears. The quasiparticle spectrum becomes fully gapped again, and κ/T vanishes at $T = 0$.

In this explanation the nodeless-nodal transition is roughly associated with the vanishing of one pair of reconstructed FS pockets. An SDW-driven electronic transition has been observed by ARPES as well as by transport measurements in electron-doped $Ba(Fe_{1-x}Co_x)_2As_2$ [26]. In that case, however, the reconstructed pocket that disappears is a much smaller hole-like pocket associated with additional details of the band dispersion not captured by our simplified two-band model. It would be interesting to verify experimentally whether the transition from four to two pockets takes place in the hole-doped $(Ba_{1-x}K_x)Fe_2As_2$ materials, and what is their relationship to the SC gap structure. Such transitions should have distinct signatures not only in the band dispersions, but also in transport coefficients. Furthermore, as discussed in Refs. 27,28, the onset of accidental nodes should also affect the low-temperature behavior of several thermodynamic quantities, giving rise to peculiar scaling relations. Another result of our analysis is the observation of a dip in the doping dependence of T_c near the doping where the system undergoes the nodal-nodeless transition.

Our model indeed does not include all aspects of the physics of the co-existence state. In particular, doping with holes or electrons changes the chemical potential, which was kept constant in our calculation. The feedback from this change affects the values M_1 and M_2 at which reconstructed pockets disappear leaving a possibility that reconstructed FSs can be present even for zero doping. The angular dependence of the magnetic interaction may also preserve FS pockets even for large M [21]. Still, we believe that the physics described by our model is quite genetic and should hold for more realistic models.

Finally, we point out that the disappearance of two out of four pockets is not the only mechanism that can give rise to nodes in the coexistence state. When the exchange interaction between unreconstructed hole and electron pockets is strong enough, it can induce nodes even in the absence of any dramatic change of the reconstructed FSs. Conversely, there is also a region in parameter space (small s) in which the coexistence with SDW does not generates nodes in the SC gap.

We are thankful to L. Taillefer, J.-P. Reid, R. Prozorov, M. Tanatar, J. Schmalian, I. Eremin, J. Knolle, for useful discussions and for sharing unpublished results with us. The work was supported by NSF-DMR-0906953 (S. M and A.V.C) and by the NSF Partnerships for International Research and Education (PIRE) program (R.M.F.). A.V.C gratefully acknowledges partial support from Humboldt foundation.

[1] K. Terashima, Y. Sekiba, J. H. Bowen, K. Nakayama, T. Kawahara, T. Sato, P. Richard, Y.-M. Xu, L. J. Li, G. H. Cao, Z.-A. Xu, H. Ding and T. Takahashi, Proc. Natl. Acad. Sci. USA **106**, 7330 (2009)

[2] K. Gofryk, A. S. Sefat, M. A. McGuire, B. C. Sales, D. Mandrus, J. D. Thompson, E. D. Bauer, and F. Ronning, Phys. Rev. B. **81**, 184518(2010).

[3] R. T. Gordon, N. Ni, C. Martin, M. A. Tanatar, M. D. Vannette, H. Kim, G. D. Samolyuk, J. Schmalian, S. Nandi, A. Kreyssig, A. I. Goldman, J. Q. Yan, S. L. Bud'ko, P. C. Canfield, and R. Prozorov, Phys. Rev. Lett. **102**, 127004 (2009).

[4] Y-M. Xu, Y-B. Huang, X-Y. Cui, E. Razzoli, M. Radovic, M. Shi, G-F. Chen, P. Zheng, N-L. Wang, C-L. Zhang, P-C. Dai, J-P. Hu, Z. Wang, and H. Ding, Nat. Phys. **7**, 198 (2011).

[5] X. G. Luo, M. A. Tanatar, J.-Ph. Reid, H. Shakeripour, N. Doiron-Leyraud, N. Ni, S. L. Bud'ko, P. C. Canfield, Huiqian Luo, Zhaosheng Wang, Hai-Hu Wen, R. Prozorov, and Louis Taillefer, Phys. Rev. B. **80**, 140503 (2009)

[6] C. Martin, R. T. Gordon, M. A. Tanatar, H. Kim, N. Ni, S. L. Bud'ko, P. C. Canfield, H. Luo, H. H. Wen, Z. Wang, A. B. Vorontsov, V. G. Kogan, and R. Prozorov, Phys. Rev. B. **80**, 020501(2009).

[7] T. Shimojima, F. Sakaguchi, K. Ishizaka, Y. Ishida, T. Kiss, M. Okawa, T. Togashi, C.-T. Chen, S. Watanabe, M. Arita, K. Shimada, H. Namatame, M. Taniguchi, K. Ohgushi, S. Kasahara, T. Terashima, T. Shibauchi, Y. Matsuda, A. Chainani, and S. Shin, Science **332**, 564 (2011).

[8] K. Hashimoto, M. Yamashita, S. Kasahara, Y. Senshu1, N. Nakata, S. Tonegawa, K. Ikada, A. Serafin, A. Carrington, T. Terashima, H. Ikeda, T. Shibauchi, and Y. Matsuda, Phys. Rev. B. **81**, 220501(2010).

[9] D. K. Pratt, W. Tian, A. Kreyssig, J. L. Zarestky, S.

Nandi, N. Ni, S. L. Bud'ko, P. C. Canfield, A. I. Goldman, and R. J. McQueeney, Phys. Rev. Lett. **103**, 087001 (2009).

[10] S. Avci, O. Chmaissem, E. A. Goremychkin, S. Rosenkranz, J.-P. Castellan, D. Y. Chung, I. S. Todorov, J. A. Schlueter, H. Claus, M. G. Kanatzidis, A. Daoud-Aladine, D. Khalyavin, and R. Osborn Phys. Rev. B. **83**, 172503(2011).

[11] M.-H. Julien, H. Mayaffre, M. Horvatic, C. Berthier, X. D. Zhang, W. Wu, G. F. Chen, N. L. Wang and J. L. Luo, Eur. Phys. Lett. **87** 37001 (2009).

[12] E. Wiesenmayer, H. Luetkens, G. Pascua, R. Khasanov, A. Amato, H. Potts, B. Banusch, H.-H. Klauss, and D. Johrendt, Phys. Rev. Lett. **107**, 237001 (2011).

[13] D. Parker, M. G. Vavilov, A. V. Chubukov, and I. I. Mazin, Phys. Rev. B **80**, 100508 (2009).

[14] A. B. Vorontsov, M. G. Vavilov, and A. V. Chubukov, Phys. Rev. B 81, 174538 (2010).

[15] R. M. Fernandes and J. Schmalian , Phys. Rev. B **82**, 014521 (2010).

[16] R. M. Fernandes and J. Schmalian , Phys. Rev. B **82**, 014520 (2010).

[17] I. Eremin and A. V. Chubukov, Phys. Rev. B 81, 024511 (2010); J. Schmiedt, P. M. R. Brydon, and C. Timm, arXiv:1108.5296.

[18] R. Fernandes *et al*, arXiv:1110.1893.

[19] A.V. Chubukov, Physica C **469**, 640 (2009).

[20] The actual situation may be more complex as at least in some orbital models SDW gap turns out to be angular dependent and vanishes along particular directions[21]. Near these directions FS survives even when SDW order parameter is large.

[21] Y. Ran, F. Wang, H. Zhai, A. Vishwanath, and D.-H. Lee, Phys. Rev. B **79**, 014505 (2009).

[22] J.-Ph. Reid, M. A. Tanatar, X. G. Luo, H. Shakeripour, S. René de Cotret, A. Juneau-Fecteau, N. Doiron-Leyraud, J. Chang, B. Shen, H.-H. Wen, H. Kim, R. Prozorov, and Louis Taillefer, arXiv:1105.2232 (2011); R. Prozorov and M. Tartar, private communication; J.-Ph. Reid and Louis Taillefer, APS March Meeting Abs: A22.00004, (2012)

[23] R. Prozorov and M. Tartar, private communication.

[24] M. G. Vavilov, A. V. Chubukov, and A. B. Vorontsov, Phys. Rev. B 84, 140502 (2011); M. G. Vavilov and A. V. Chubukov, arXiv:1110.0972

[25] Y. Zhang, E. Demler, and S. Sachdev, Phys. Rev. B. **66**, 094501 (2002)

[26] C. Liu *et al.,* Nature Phys. **6**, 419 (2010).

[27] Valentin Stanev, Boian S. Alexandrov, Predrag Nikolic, and Zlatko Tesanovic, Phys. Rev. B **84**, 014505 (2011).

[28] R. M. Fernandes and J. Schmalian, Phys. Rev. B **84**, 012505 (2011).